

Study of ferrofluids by Mössbauer spectroscopy

H.-D. Pfannes^a, J.H. Dias Filho^a, J.L. López^a, S.L. Pereira^a, P.C. Morais^b
and F.A. Tourinho^b

^a *Departamento de Física, Universidade Federal de Minas Gerais, C.P. 702,
30123-970 Belo Horizonte, Brazil*

^b *Departamento de Física, Universidade de Brasília, 70910 Brasília, Brazil*

The parameters of the log-normal size distribution of a MnFe_2O_4 ferrofluid powder sample have been determined by X-ray diffraction. The mean blocking temperature was determined from the maximum of $\chi_i(T)$. Mössbauer spectra at 4.2–300 K are interpreted by a new simple theory of superparamagnetism and taking a reduction of the internal magnetic field for small particles, a size dependence of the anisotropy constant, the size distribution and collective excitations into account.

1. Introduction

Ferrofluids consist of stable colloidal suspensions of nanometer-sized magnetic particles (ionic type or coated with surfactant layers) in a non-magnetic carrier liquid. Due to their unique properties they find numerous technological applications, e.g., as printer ink, rotary vacuum-seals, loudspeaker cooling, drug-carrier in chemotherapy, etc. Besides that, ferrofluids or powders of their constituents (normally monodomain ultra-fine particles of spinel-type ferrites) are interesting in fundamental research because of their nano-scale dimensions. In their magnetic behaviour phenomena like superparamagnetism or even spin-tunneling [1,2] may be involved.

Besides other methods, like small angle neutron scattering, magnetic resonance and optical methods, studies of the magnetic properties of ferrofluids are advantageously realized by Mössbauer spectroscopy (see, e.g., [3–7]), which may also give information on valence states, site occupations and internal magnetic fields, and dc- or ac-magnetometry (see, e.g., [7,8]). The two methods differ in their characteristic times which are approximately 100 s or 10^{-3} – 10^{-4} s for dc- or ac-magnetometry, respectively, and 10^{-9} s for Mössbauer spectroscopy. We present here results on dc-magnetometry and Mössbauer spectroscopy of Mn-ferrite. The Mössbauer results are interpreted by a new simple model of superparamagnetism.

2. Experimental

Ferrofluids of Mn-ferrite (MnFe_2O_4) and other ferrites have been produced by chemical synthesis (coprecipitation of MnCl_2 , $\text{Co}(\text{NO}_3)_2$ and NiCl_2 with FeCl_3 in

alkaline medium) of the corresponding nanoparticles with subsequent peptization by an appropriate particle surface treatment [9]. Thus water-based ionic ferrofluids with different average particle diameters, depending on the coprecipitation conditions, are obtained. Here we report only on Mn-ferrite based samples (powder sample and the corresponding ferrofluid). Results of the investigation of Co-, and Ni-ferrites will be reported elsewhere.

Powder samples as obtained before the peptization and frozen ferrofluids have been analyzed by X-ray diffraction (Rigaku Geigerflex powder diffractometer, Cu-radiation, graphite monochromator between sample and detector), vibrating sample magnetometry (VSM, PAR 4500 with Janis cryostat and superconducting magnet, 0–90 kOe, 2–300 K), differential scanning calorimetry (DSC, Mettler 3000) and Mössbauer spectroscopy (constant acceleration spectrometer, source: ^{57}Co in Rh).

3. Results

3.1. X-ray diffraction

Part of an X-ray diffraction pattern of the Mn-ferrite powder sample is shown in figure 1. All main peaks of the patterns could be identified and there was no indication of the presence of other compounds. The lattice constant was determined to $(8.400 \pm 0.001) \text{ \AA}$.

From electron micrographs of identically prepared samples [5,9] was concluded that the particles are approximately spherical and that their size distribution $p(D)$ obeys a log-normal relation

$$p(D) = \frac{1}{(2\pi)^{1/2}\sigma D} \exp\left(-\frac{(\ln(D/D_0))^2}{2\sigma^2}\right), \quad (1)$$

where D is the particle diameter, D_0 the median D and σ the standard deviation of $\ln(D/D_0)$. From the width of the main (3 1 1)-line of the X-ray diffraction pattern, comparing to a Si-standard, we calculated $D_0 = 9.045 \text{ nm}$ (cf. figure 1).

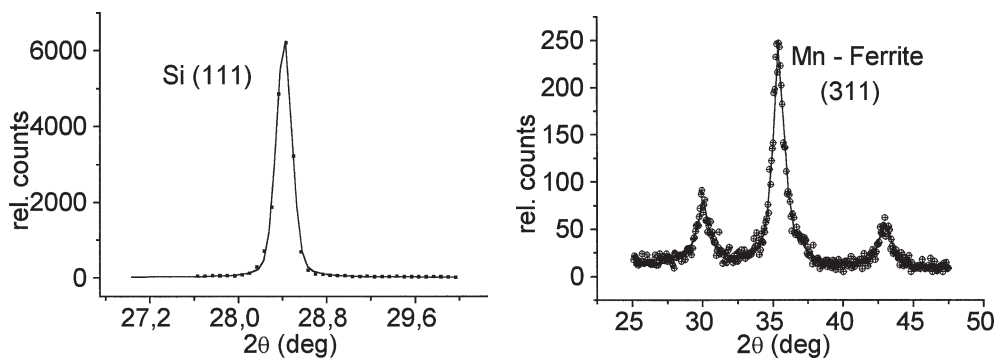


Figure 1. X-ray diffraction pattern of Mn-ferrite and Si-standard.

3.2. Magnetic measurements

From $M(H)$ -measurements ($H = 0\text{--}20$ kOe) at constant temperatures $T = 4.2\text{--}300$ K the reduced magnetization M/M_s as function of H/T has been derived. The curves for $T = 250$ K and 300 K superimpose and could be successfully fitted by a Langevin function $L(y)$ weighted with the particle size distribution using $D_0 = 8.0$ nm and $\sigma = 0.28$ according to

$$M(H/T) \propto \int \mu L(y) p(\mu) d\mu, \quad (2)$$

where $\mu = M_s V$, $y = \mu H/k_B T$, k_B is Boltzmann's constant, $V = \pi D^3/6$ is the volume of a particle and the saturation magnetization M_s has been obtained by extrapolating $M(1/H)$ -curves to $1/H = 0$. The superposition of the curves clearly indicates superparamagnetic behavior within the time window of the VSM method.

In figure 2 the dependence of the initial susceptibility χ_i on temperature is shown. A broad maximum at a temperature of $T_g \approx 75$ K can be observed. T_g is related to the mean blocking temperature $\langle T_B \rangle$ defined by

$$\langle T_B \rangle = (K V_0/k_B) \ln(\tau/\tau_0), \quad (3)$$

where τ is the characteristic time of the measuring method (here ≈ 100 s), $\tau_0 \approx 10^{-9}$ s, $V_0 = \pi D_0^3/6$ and K the magnetic anisotropy constant of the particles, here assumed to possess uniaxial anisotropy and size independent K . $\langle T_B \rangle$ is proportional to T_g and the proportionality constant depends on the size distribution $p(D)$. The proportionality constant is unity for unique particle size and 2 for a rectangular distribution [10]. We calculated it from the log-normal distribution with $D_0 = 8.0$ nm and $\sigma = 0.28$ and obtained a value of 1.58 and thus from the susceptibility maximum $\langle T_B \rangle \approx 48$ K.

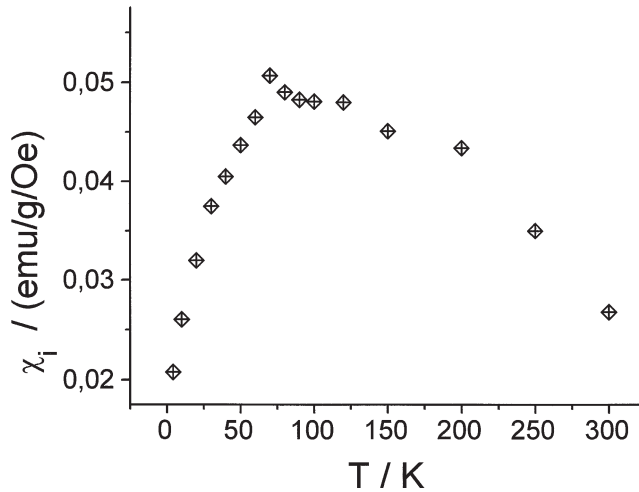


Figure 2. Initial susceptibility as function of temperature.

3.3. Mössbauer spectroscopy

Mössbauer spectra of the powder sample at temperatures in the range of 4.2–295 K are shown in figure 3(d). The corresponding ferrofluid with smaller particle concentration exhibits similar spectra. The upper spectrum at $T = 340$ K, shown for comparison with simulations, was taken from [5] and refers to a similar sample as ours but with $D_0 = 10$ nm.

The spectrum at 4.2 K can be satisfactorily fitted with two magnetic subspectra with internal fields H_{int} of 49.9 kOe and 52.3 kOe and an area ratio of 0.9 : 1,

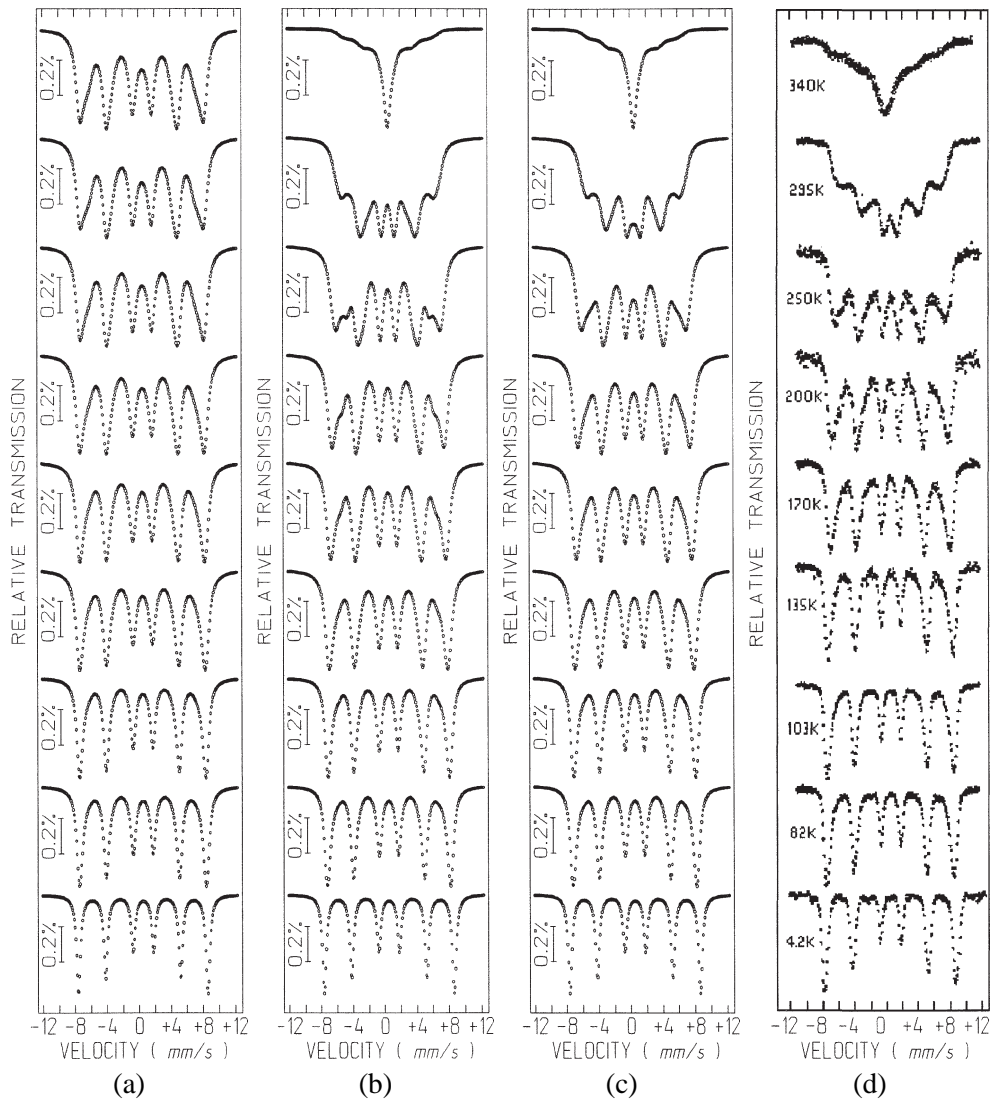


Figure 3. Simulated (a)–(c) and experimental (d) spectra. See text.

respectively. In the frame of a simple cation distribution model $(\text{Mn}_{1-x}^{2+}\text{Fe}_x^{3+})(\text{Mn}_x^{2+}\text{Fe}_{2-x}^{3+})\text{O}_4$ with tetrahedral (A)-sites and octahedral [B]-sites, respectively, and ascribing the lower field to (A)-sites this area ratio would mean $x = 0.9$, i.e., nearly complete inverse spinel. However this fit model is highly oversimplified [3]. At higher temperatures asymmetric line broadening and a broad background and central peak appear due to the effects discussed below.

It is not easy to fit consistently the spectra of figure 3(d). Assuming a simple superparamagnetic relaxation model leads to great discrepancies between experimental data and simulated spectra in the inner part of the spectral pattern (velocities of $\approx (-4)$ – $(+4)$ mm s^{-1}). Similar simulation defects can be observed, e.g., in [7,12].

4. Discussion

4.1. New model for superparamagnetism

In view of the discrepancies between the experimental spectra and simulations using collective excitations [4] and

$$\tau = \tau_0 \exp(KV/k_B T) \quad (4)$$

for the superparamagnetic relaxation time τ and considering that Brown's theory [11] is a phenomenological theory relying on statistical mechanics, we tried a simple microscopic approach based on spin-Hamiltonians. We assume that the thermally excited turnover of the magnetization in monodomain fine particles happens by coherent rotation of the spins because of predominant exchange interaction (Stoner–Wohlfarth model [13]). Thus the magnetization can be considered as due to a large spin ($S = 10^2$ – 10^4). This spin interacts with the thermal vibrations via spin–phonon coupling. This has already been proposed by Jones and Srivastava [14], however they did not present a corresponding calculation.

When no external magnetic field is present and with the assumption of uniaxial anisotropy the minima of the anisotropy energy correspond to spin states $|m\rangle = |-S\rangle$ or $|+S\rangle$ belonging to the same eigenenergy. Superparamagnetic relaxation consists then in exciting the spin S from state $|+S\rangle$ until it comes up to $|0\rangle$ with subsequent downward transitions until it reaches $|-S\rangle$. The classical anisotropy energy $E(\Theta) = KV \sin^2 \Theta$ (Θ = angle between spontaneous magnetization and anisotropy direction) corresponds to a Hamiltonian $H_S = -dS_z^2$, where $d = KV/S^2 = \Delta/S^2$ (barrier height $\Delta = dS^2$) with eigenvalues $E_m = -dm^2$ and eigenstates $|m\rangle$. The spin–phonon interaction is described by a simplified dynamical spin-Hamiltonian. We introduce the Debye-model in the long-wavelength limit, calculate the transition probabilities $W_{m,n}$ for a transition $|m\rangle \rightarrow |n\rangle$ and establish the corresponding master equation for the population of the m th level in the stationary case (for details see [15,16]). In contrary to [15,16] we admit transitions $|S\rangle \rightarrow |S-n\rangle \rightarrow |S-2n\rangle \rightarrow \dots$ where n can be $1, 2, \dots, S$. This corresponds to highly non-linear terms in the spin–phonon interaction and long-wavelength phonons with sufficiently long correlation times [17].

For superparamagnetic relaxation the processes with $n \sim S$ may be relatively probable at $T \geq T_B$, in contrast to paramagnetic relaxation where $n = 1, 2$. Similarly as in [15,16] we obtain for the probabilities p_S and p_{-S} to find a particle in the state $|S\rangle$ or $| -S\rangle$, respectively, the rate equation

$$\frac{d}{dt}(p_S - p_{-S}) = -\frac{p_S - p_{-S}}{\tau_n}$$

with the relaxation time

$$\tau_n = \frac{1}{2} \sum_{q=0}^{2S-n} \frac{\exp((E_{S-q} - E_S)/k_B T)}{W_{S-q, S-q-n}} \approx \frac{\exp((E_0 - E_S)/k_B T)}{W_{0, -n}}, \quad (5)$$

where the approximation holds for $n \sim S$. We use the expression

$$W_{m,n} = \frac{3C^2}{2\pi\hbar^4\rho v^5} (E_m - E_n)^3 \frac{1}{1 - \exp(-(E_m - E_n)/k_B T)}, \quad (6)$$

which is valid for phonon creation (spin transition from $|m\rangle \rightarrow |n\rangle$). C is a spin-phonon coupling constant and ρ and v are the density and sound velocity, respectively, of the particle. With this we obtain

$$\tau_n \approx \frac{2\pi\rho v^5 \hbar^4}{3C^2 k_B} \frac{S^4}{n^4 \Delta^2 T} \exp(\Delta/k_B T) = \tau_{0n} \exp(\Delta/k_B T). \quad (7)$$

τ_n exhibits the typical exponential dependence of superparamagnetic relaxation. The prefactor differs by n^{-4} from the prefactor calculated in [16] where only transitions $|S\rangle \rightarrow |S-1\rangle \rightarrow |S-2\rangle \rightarrow \dots$ have been taken into account. In a first tentative we take $n = S$ and for reasonable values of the parameters involved ($\Delta = 2.9 \times 10^{-20}$ J, $\rho = 5$ g cm $^{-3}$, $v = 3000$ m s $^{-1}$, $T = 300$ K and $C = 0.5$ cm $^{-1}$) we obtain $\tau_{0n} \approx 9.1 \times 10^{-10}$ s in accordance with the usual range. The prefactor τ_0 as calculated by Brown depends on temperature as $T^{1/2}$, which seems to be unphysical in the limit $T \rightarrow 0$, whereas ours as T^{-1} .

4.2. Simulation of spectra

The experimental spectra collapse very rapidly in the range of 250–340 K without showing initially a pronounced central peak. There should be another cause of internal field reduction besides increasing relaxation frequency.

DSC measurements of our sample exhibit a broad peak at ≈ 350 K which may be related to its mean Néel temperature T_N . For an inversion degree of $x = 0.9$ a value of $T_N \approx 400$ K for $D = 15.5$ nm is given in [18]. We adopted a linear dependence of T_N on the particle diameter (cf. figure 4) given by $(T_N [\text{K}]) = 8.75(D [\text{nm}]) + 264$, where $T_N(9.05 \text{ nm}) = 343$ K and $T_N(15.5 \text{ nm}) = 400$ K (the bulk value is 573 K). For each diameter D we obtain T_N and from this and the actual temperature T we get an internal magnetic field value corresponding to the variation of the internal field dependence shown in figure 5 which was obtained from the hyperfine field dependence given in [3].

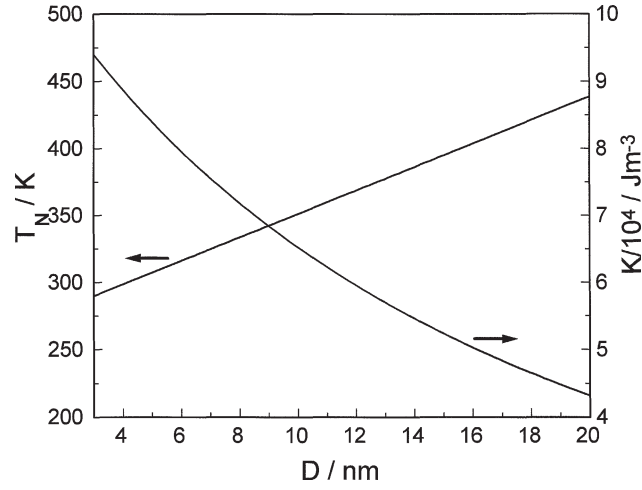


Figure 4. Néel temperature T_N and anisotropy constant K vs. diameter used in the simulations.

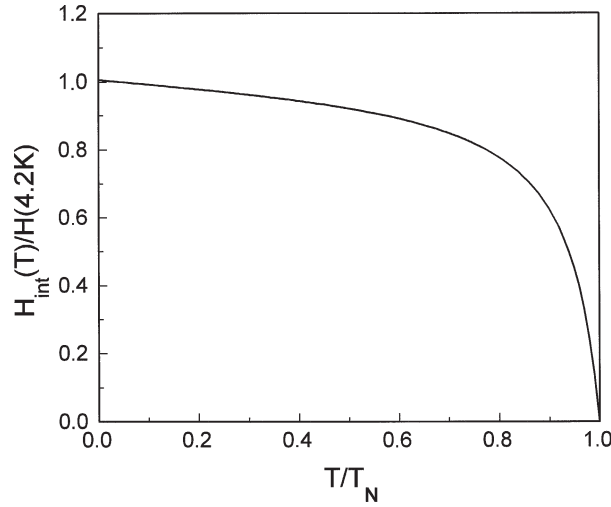


Figure 5. Reduced internal hyperfine field as function of reduced temperature [3].

We simulated Mössbauer spectra using a stochastic Clausen–Blume formalism where τ^{-1} enters as relaxation frequency. We take also a size dependence of the anisotropy constant as

$$K = (4 \times 10^3 \text{ [J m}^{-3}\text{]}) + \frac{98 \times 10^6}{((D \text{ [nm]}) + 30)^2}$$

into account (see figure 4). This dependence tends to the bulk value for $D \rightarrow \infty$ and follows the same power law as can be extracted from data given for Fe particles in [19]. Figure 3(a) shows simulations using eq. (4) with $\tau_0 = 10^{-9}$ s, $K(D_0) = 6.8 \times 10^4 \text{ J m}^{-3}$ and eq. (1) with $D_0 = 9.045 \text{ nm}$, $\sigma = 0.35$ and constant H_{int} as well as collective

excitations. For simplification we used only a single internal field $H_{\text{int}} = 50.4$ kOe and line widths of 0.6 mm s^{-1} ($T = 4.2$ K), 0.8 mm s^{-1} ($T = 82, 103$ K) and 1 mm s^{-1} ($T \geq 135$ K) to take the crossover of the various H_{int} [3,6] in the whole temperature region into account. The relative line intensities have been chosen according to the 4.2 K spectrum and fixed for all temperatures.

Due to the appearance of a strong central peak when using other parameters it was not possible to obtain a better agreement of the simulations with the experimental spectra. In figure 3(b) the reduction of H_{int} according to figures 4 and 5 and a prefactor $(T/T_0)^{1/2}$ according to Brown [11] is included, where $T_0 = 4.2$ K is chosen to obtain a good simulation of the static spectrum. However one clearly remarks that the simulations in the temperature range 200–295 K do not reproduce well the experimental spectra. Figure 3(c) shows simulations using the same parameters as in figure 3(b) and a prefactor $((4.2 \text{ [K]})/T) \times 10^{-9}$ s according to our model. A good correspondence with the experimental spectra in the whole temperature range with one unique consistent set of τ_0 , D_0 , σ , $T_N(D)$ and $K(D)$ is observed.

Using eq. (4) with the prefactor $\tau_0 = ((4.2 \text{ [K]})/T) \times 10^{-9}$ s, a medium $K = 6.8 \times 10^4 \text{ J m}^{-3}$ and $\tau = 100$ s for the magnetic measurements we obtain $D_0 = 8.02$ nm for $T = \langle T_B \rangle = 48$ K, consistent with that derived from magnetic measurements. The smaller D_0 may indicate that spin-pinning occurs in the surface region of the particles, resulting in a smaller “magnetic volume” [20].

Acknowledgement

The support of the Brazilian agencies CNPq, FAPEMIG and FINEP is gratefully acknowledged.

References

- [1] C.P. Bean and J.D. Livingston, *J. Appl. Phys.* 30 (1959) 120S.
- [2] D.D. Awschalom and D.P. DiVincenzo, *Physics Today*, April 1995, 43.
- [3] G.A. Sawatzky, F. Van der Woude and A.H. Morrish, *Phys. Rev.* 187 (1969) 747.
- [4] S. Mørup and H. Topsøe, *Appl. Phys.* 11 (1976) 63.
- [5] H.R. Rechenberg and F.A. Tourinho, *Hyp. Interact.* 67 (1991) 627.
- [6] E. Wieser, W. Meisel and K. Kleinstück, *Phys. Status Solidi* 16 (1966) 127.
- [7] A. Tari, J. Popplewell, S.W. Charles, D.St.P. Bunbury and K.M. Alves, *J. Appl. Phys.* 54 (1983) 3351.
- [8] H.D. Williams, K. O’Grady, M. El-Hilo and R.W. Chantrell, *J. Magn. Mater.* 122 (1993) 129.
- [9] F.A. Tourinho, R. Franck and R. Massart, *J. Mater. Sci.* 25 (1990) 3249.
- [10] J.I. Gittleman, B. Abelas and S. Bozowski, *Phys. Rev. B* 9 (1974) 3891.
- [11] W.F. Brown Jr., *Phys. Rev.* 130 (1963) 1677.
- [12] S. Mørup, H. Topsøe and J. Lipka, *J. Physique Colloq.* 37 (1976) C6-287.
- [13] E.C. Stoner and E.P. Wohlfarth, *Philos. Trans. Roy. Soc. London Ser. A* 240 (1948) 599; reprinted in *IEEE Trans. Magn.* 27 (1991) 3475.
- [14] D.H. Jones and K.K.P. Srivastava, *Phys. Rev. B* 34 (1986) 7542.

- [15] J. Villain, F. Hartmann-Boutron, R. Sessoli and A. Rettori, *Europhys. Lett.* 27 (1994) 159.
- [16] H.-D. Pfannes, *Hyp. Interact.* 110 (1997) 127.
- [17] D.H. Jones and K.K.P. Srivastava, *J. Magn. Magn. Mater.* 78 (1989) 320.
- [18] R.V. Upadhyay, K.J. Davies, S. Wells and S.W. Charles, *J. Magn. Magn. Mater.* 132 (1994) 249.
- [19] S. Gangopadhyay, G.C. Hadjipanayis, B. Dale, C.M. Sorensen, K.J. Klabunde, V. Papaefthymiou and A. Kostikas, *Phys. Rev. B* 45 (1992) 9778.
- [20] A.E. Berkowitz, J.A. Lahut, I.S. Jacobs, L.M. Levinson and D.W. Forester, *Phys. Rev. Lett.* 34 (1975) 594.